Review Article

Journal of Applied Material Science & Engineering Research

Controllable Synthesis and Luminescent Property of Europium-Based Metal-Organic Frameworks

Bangyu Chen, Ting Yang, Li Feng, Yue Li, Yang Deng, ZiruoZou, Xin Lai and ZhangleiNing*

College of Chemistry and Materials Science, Sichuan Normal University, Chengdu 610068, China

***Corresponding author**
ZhangleiNing, College of Chemistry and Materials Science, Sichuan Normal University, Chengdu 610068, China, Tel: +86-18980993165; E-mail: zlnn2008@126.com; zlning@sicnu.edu.cn

Submitted: 16 Mar 2018; **Accepted**: 02 Apr 2018; **Published**: 20 Apr 2018

Abstract

Elllipse-like europium-based metal–organic framework (MOF) has been successfully synthesized on a large scale through an efficient and facile direct precipitation method. The composition and structure of the samples were well characterized by Fourier transform infrared spectroscopy (FTIR), X-ray powder diffraction (XRD), elemental analysis (EA), scanning electronic microscope (SEM), and photoluminescent spectra (PL), respectively. The speculated molecular formula of the Eu-based MOF is $[Eu(MA)_{1.5}(H_2O)_2]\bullet 5H_2O$. The experimental result demonstrate that these elllipse-like with diameter of about 3-5 μm are assembled of a series of dense nanoplate. The effect of MA/KOH molar ratio and surfactant on the morphologies and sizes of the final microcrystals were studied. Moreover, the morphology-dependent photoluminescence properties were also investigated in detail. This preparation route is very prospective for the synthesis of the other nano/micro-sized materials due to its simple synthesis method.

Keywords: Metal-Organic Framework, Morphology, Luminescent

Introduction

Nowadays, metal–organic frameworks (MOFs) from metal ions with organic bridging ligands have acquired tremendous attention attribute to their diversified structure and potential appliances in gas storage, photo-catalysis, chemical sensor, phosphor, and applications [1-4]. It is worth noting that the lanthanide metal-organic frameworks (Ln-MOFs) has excellent luminescent properties due to superior vitality and multi-coordination structure, such as large stokes migration, long fluorescence lifetime,efficient selectivity for probe identify [5-7]. Ligand sensitization lanthanide luminescence is called "antenna effect" or "luminescence sensitization", the mechanism is that the organic ligand coordinated with the metal ion absorbs UV or near ultraviolet radiation and then transfers the energy to attached Ln (I II) ions [8,9]. Given the unique and commendable luminescence properties, Ln-MOFs have been used in many applications such as cations, anions, small molecules, and explosives [10-19]. Nonetheless, there are few reported on the morphology control growth and their formation mechanisms of Ln-MOFs. Ln-MOFs have been developed only a few preparation methods, including template, hydrothermal and solvothermal synthesis, and so on [20,21]. However, most of these methods require longer reaction time, complicated conditions and higher costs, which greatly limit their application prospects. Therefore, it is necessary to develop a simple, rapid, and cost-effective method to prepare nano- and microscale lanthanide metal-organic framework.

As we known, Eu^{3+} is an excellent red-emitting activator attribute to their particular energy level structure and the plentiful 4f-4f and 5d-4f transitions [22,23]. Mucic acid (MA) plays an important part in life science, it is also a multi-functional multidentate chelator that consist of four hydroxyl groups and two carboxyl along the carbon chain, which may resulting in a variety of coordination modes and the formation of multiple structures [24,25]. Until now, metal based mucic acid MOFs have been reported [26-29]. However, there have been few reports mentioning about nano/micro-sized lanthanide mucic acid MOF materials. Moreover, a lot of research has been devoted to adjusting the shape and size of the sample to control its application. Although, the physical and chemical properties of the fuctional materials greatly depend on the their morphology, phase, shape, size, distribution, as well as their composition.

Hence, in this work, we report on novel design the system of europium-based metal-organic framework via an efficient and facile method at room temperature. More importantly, the effect of Eu/KOH molar ratio and surfactant on the morphology of the samples were studied. The composition, morphology, and photoluminescence properties of the products were also investigated in detail.

Experimental section

Preparation of Eu-MOFs

A series of microstructures europium metal-organic frameworks were synthesized, mucic acid (MA) was dissolved in 20 mL distilled water system under agitated stirring to get a transparent solution, a certain amount of KOH aqueous was added into the above solution at room temperature. After vigorous stirring for 30 min, quantitative surfactants were added to the mixture. Then 8 mL of 0.025 M

$Eu(NO_3)_3$•$6H_2O$ solution was added into the solution under stirring. After additional agitation for 30 min, the resulting precipitations were separated by centrifugation, washed several times with distilled water and absolute ethanol, and finally dried under oven at 55°C.

Characterization

Fourier transform infrared spectroscopy (FTIR) spectrum was obtained on NEXUS 670 (Nicolet, America). The spectrum was recorded in the 4000-400 cm^{-1} region by using pressed KBr tables. The powder X-ray diffraction (XRD) data were examined on the Rigaku Smart Lab X-ray diffraction with Cu K_a radiation (λ = 0.15406 nm) at a scanning rate of 8°/min in the 2θ range from 5° to 70°. Elemental analysis of C, and H in the solid samples was carried out on EA 3000 (EuroVector). The morphology of the samples was examined on a Quanta 250 scanning electron microscope (SEM). The luminescent excitation and emission spectra (PL) were acquired on a F-7000 fluorescence spectrophotometer equipped with a 150 W xenon lamp as the excitation source. All measurements were performed at room temperature.

Results and Discussion

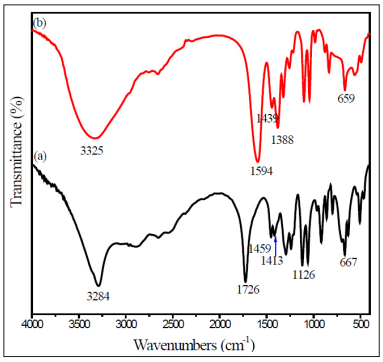

Figure 1: FTIR spectra of MA (a) and Eu-based metal-organic framework (b)

FTIR spectra were firstly used to investigate the chemical composition of the ligand (mucic acid, MA) and as-synthesized Eu-based metal-organic frameworks. From Figure 1, it can be clearly seen that the characteristic bands of the nonionized carboxyl group of MA disappear (1726 cm^{-1}) and new bands observed at 1594 and 1388 cm^{-1} which are attributed to the asymmetric and symmetric stretching vibration of the ionized carboxyl group [30,31]. It proves that the Eu^{3+} ions have been coordinated with the mucic acid ligands successfully. In addition, the broad band centered at 3325 cm^{-1} should be the stretching vibration of -OH, indicating that water molecules exist in the structure of the Eu-based metal-organic frameworks.

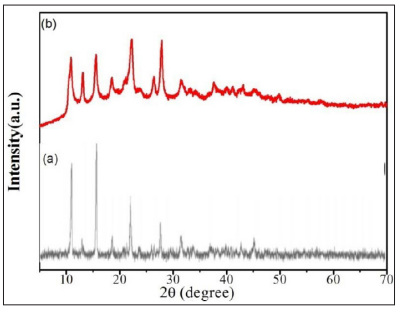

Figure 2: XRD patterns of reported $[Tb(MA)_{1.5}(H_2O)_2]\cdot 5H_2O$ crystal (a) and the as-obtained EuMA samples (b)

To further investigate the chemical composition and crystal structure of Eu-based metal-organic frameworks products, X-ray powder diffraction (XRD) were characterized. As shown in Figure 2, it can be seen that the as-obtained samples present high crystallinity in spite of the moderate reaction conditions (such as room temperature reaction, 30 min). All the displayed diffraction peaks can be well indexed to the known crystal phase of $[Tb(MA)_{1.5}(H_2O)_2]$•$5H_2O$, demonstrating that the as-synthesized product is identical structural with this reported structure [32]. So the products can be presumed to be a composition of $[Eu(MA)_{1.5}(H_2O)_2]$•$5H_2O$ (EuMA). No peak shift and other phases can be detected in the XRD patterns, indicating that the pure EuMA crystals have been obtained by this method. Moreover, elemental analysis was also studied. The experimental contents of C and H are shown to be 19.91 and 3.62%, respectively, which are basically in consistent with theoretical datas of C (18.49%) and H (3.42%), confirming the molecular formula of the europium-based MOF is $[Eu(MA)_{1.5}(H_2O)_2]$•$5H_2O$.

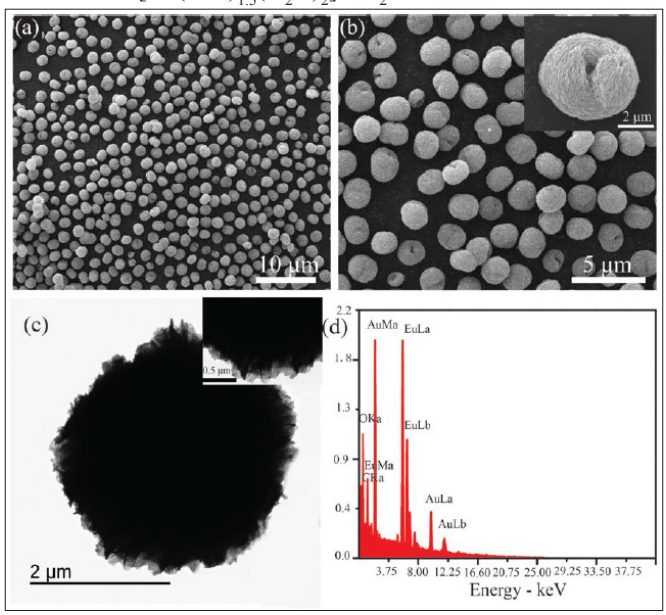

Figure 3: SEM images (a, b) and TEM images (c)and EDX spectrum (d) of EuMAsamples

The morphology and structural features of the as-synthesized EuMA products were characterized using scanning electron microscopy (SEM) and transmission electron microscopy (TEM). Figure 3a displays a representative overview of the samples. It can be seen that the products consist of uniform and well-dispersed 3D ellipse-like structures with lengths of about 3 to 5 μm on a large scale. The magnified SEM image shown in Figure 3b reveals that the ellipse-like is composed of a great deal of dense nanoplates with a thickness of about 50 nm. In addition, this elliptical structure of the as-obtained EuMA samples could not be destroyed and broken into discrete nanoplates even by ultrasonically treating for 30 min, indicating that the structures are not a random aggregate but the ordered self-assembly of the nanoplates. Figure 3c show the low-and high magnification TEM images. It can be seen that the nanoplates are assembled in a radial form from the center to the surface of ellipse-like EuMA samples. The EDX spectrum (Figure 3d) of the EuMA products demonstrate the presence of C, O, and Eu(Au from the coating for SEM measurement), which is in agreement with the aboved composition analysis. This further verifys that the expected products have been synthesized successfully by introducing the

solution of $Eu(NO_3)_3$ into the mucic acid solution under stirring at room temperature.

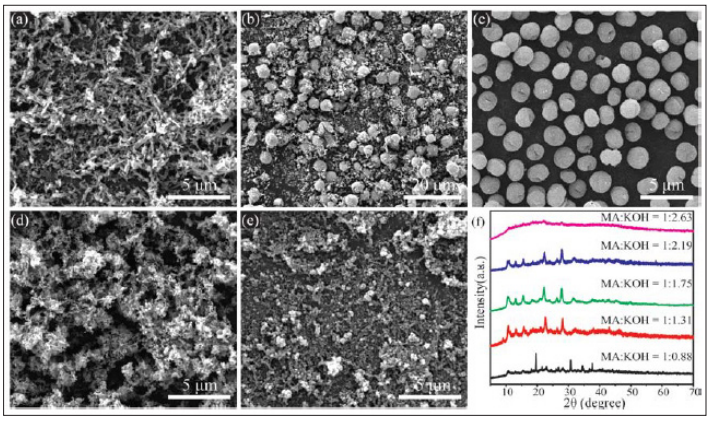

Figure 4: SEM images of EuMA samples prepared with different MA/KOH molar ratios: (a) 1:0.88; (b) 1:1.31; (c) 1:1.75; (d) 1:2.19; (e) 1:2.63; (f) XRD patterns of these samples

Figure 4 illustrates the SEM images and XRD pattern of the as-obtained EuMA samples synthesized at different MA/KOH molar ratios. It is apparent that the samples present distinctly different morphologies during crystal growth. When the MA/KOH molar ratios is 1:0.88, the final products exhibit nanorods with an averge length of 500 nm and a width of about 100-200 nm (Figure 4a). As molar ratio decreases to 1:1.31, the samples consist of lots of nanorods with an average size of 500 nm and some ellipse-like particles appeared (Figure 4b). When molar ratio decreases to 1:1.75 (Figure 4c), samples become regular and dispersive, and ellipse-like particles with the average size of about 3-5 μm are obtained. Further decrease the molar ratio to 1:2.19, some irregular nano-sized particles can be observed (Figure 4d). Meanwhile, with molar ratio further decreasing to 1:2.63, all the products show irregular flocculent nanoparticles (Figure 4e). It is obvious that MA/KOH molar ratios should be responsible for the morphology of EuMA products and a moderate molar ratio is more effective for the formation of the elliptical EuMA samples.

As shown in Figure 4f, the effect of MA/KOH molar ratios on the crystal structure of EuMA was studied by XRD. It is can be seen that the MA/KOH molar ratios had pivotal influences on the formation of EuMA phase. At the MA/KOH molar ratios was 1:0.88, the XRD pattern of the samples are weak and unique, and no reported crystal can be indexed. We speculate that it is a new crystal phase of EuMA. The new complexes formed by the Eu^{3+}cations and the Cit3- anions. When the MA/KOH molar ratios lower than 1:1.31, all the diffraction peaks of the as-prepared samples can be coincide the phase of $[Tb(MA)_{1.5}(H_2O)_2]\bullet 5H_2O$. However, as the MA/KOH molar ratios decrease to 1:2.63, there is no other diffraction peaks of phases, indicating that the samples are amorphous and not crystalline.

From the above experimental results, it can be found that the MA/KOH molar ratios play an important role in the formation of pure phase and regular morphology of the final products. The well-crystallized ellipse-like EuMA microcrystals can be synthesized at appropriate MA/KOH molar under the room temperature. It is well known that the growth process of crystals can be classified into two steps: an initial nucleating stage and a crystal growth stage. At the first stage, the formation of the crystal nucleus is crucial for further growth of the crystals. The second crystal growth stage is a kinetically and thermodynamically controlled process. In our case, mucic acid is a typical multi-carboxylic acid ligands and KOH is a representative strong alkali. In the present of KOH, MA can turn into carboxylate. And carboxylate ions in the solution will react with Eu^{3+} cations to form EuMA nuclei duo to their strong coordination. Thus, the MA/KOH molar would greatly effect the concentration of carboxylate ions and further change the nucleation rate of crystal. Moreover, at higher or lower MA/KOH molar, excessive carboxylate ions will selective adsorb on certain crystal planes due to electrostatic interaction. As a result, the reactivity and the growth rate of high-energy facets will be reduced. Therefore, the nucleation and growth behavior would be out of kinetic control and the final products tend to be irregular and impure. On the basis of the above analyses, well-crystallized EuMA microcrystals with different morphologies can be selectively synthesized by judicious choice of MA/KOH molar ratios.

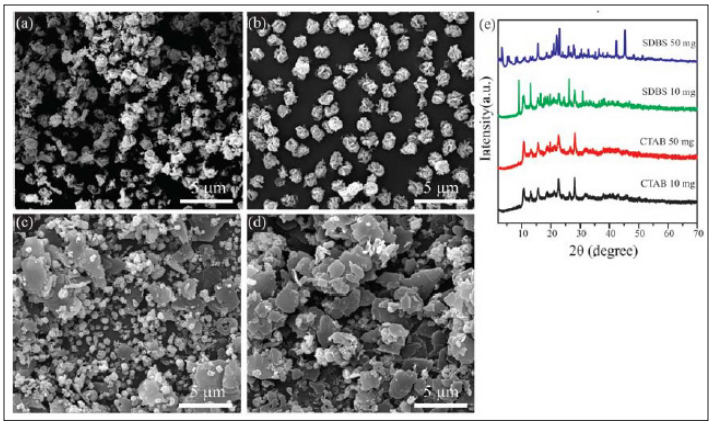

Figure 5: SEM images of EuMA samples synthsized with different amounts of surfactants: (a) CTAB 10 mg; (b) CTAB 50 mg (c) SDBS 10 mg; (d) SDBS 50 mg; (e) XRD patterns of these samples

Moreover, some surfactants, such as cetyltrimethyl ammonium bromide (CTAB) and sodium dodecyl benzene sulfonate (SDBS) were also introduced individually into the reaction system. Figure 5 shows the SEM images of the as-synthesized samples prepared by adding different amount of CTAB (Figure 5a-b) and SDBS (Figure 5c-d), respectively. It can be seen that the morphologies of the as-synthesized samples are changed significantly. As shown in Figure 5a, when a small amount of CTAB (10 mg) was added, irregular spherical particals were obtained. Interestingly, when further increase CTAB to 50 mg, well-defined uniform flower-like microcrytals with size of about 2-3 μm are observed in the SEM images (Figure 5b). Meanwhile, pure phase without impurity phases are detected in the corresponding XRD patterns (Figure 5f). Figure 5c-d show the SEM images of samples synthesized by using SDBS as an organic additive. The product consist of ellipse-like and plate-like microparticles with irregular shape when the content of SDBS is 10 mg. Interestingly, further increase the content of SDBS to 50 mg, the plate-like microstructures with the size of 2-8 μm were dominant in the products. The XRD pattern show impurity peaks observed and no matched reported crystal was found. These results indicate that the organic additives have a remarkably different impact on the morphologies and crystal structure of the final EuMA products, which is related to the differences of the chelating constant with Eu^{3+} and the adsorption ability of the different crystal facets of the final products [33-34]. This facile, mild and cost-effective growth

strategy may serve as guidance for the synthesis of other nano/micro metal-organic materials with uniform and novel morphologies.

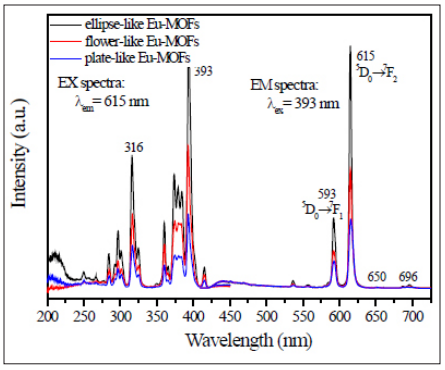

Figure 6: Morphology-dependent excitation and emission spectra of EuMA samples

The photoluminescence properties of EuMA samples with different morphology were investigated in detail. Figure 6 shows the room-temperature PL excitation and emission spectra of EuMA with ellipse, flower, plate-like morphology. It is apparent that all the excitation and emission spectra of these three samples are similar in shape, but different in the intensity to some extent. The excitation spectrum (EX) was obtained by monitoring the emission of the $^5D_0$-$^7F_2$ transition of the Eu^{3+} ions at 615 nm. It can be easily seen that the excitation spectrum consists of several lines in the range from 250 to 450 nm. The strong lines at 316, 364, 384, 393, and 418 nm are contributed to the $^7F_0$-$^5H_6$, $^7F_0$-$^5D_4$, $^7F_0$-^5G_J, $^7F_0$-$^5L_6$, and $^7F_0$-$^5D_3$ transitions of Eu^{3+}, respectively [34]. The most intense peak appear at 393 nm, which are assigned to the transition between $^7F_0$ and $^5L_6$.

The emission spectra show peaks from the excited state $^5D_0$ to ^7F_J (J =1, 2, 3, 4) of the Eu^{3+} ion electron energy levels. Upon the excitation at 393 nm, the emission spectrum (EM) of the as-obtained sample shows several sharp lines from 550-700 nm, which can be attributed to $^5D_0 \rightarrow ^7F_1$ (593 nm), $^5D_0 \rightarrow ^7F_2$ (615 nm), $^5D_0 \rightarrow ^7F_3$(650 nm), $^5D_0 \rightarrow ^7F_4$ (696 nm) of Eu^{3+} [35]. It is well known that Eu^{3+} ions are universally structure probes to investigate the local environment in crystal. If the electric dipole transition $^5D_0/^7F_2$ (615 nm) is dominant, the Eu^{3+} ions occupy sites without inversion symmetry; however, when the magnetic dipole transition $^5D_0/^7F_1$ (593 nm) is dominant, the Eu^{3+} ions are in the sites of inversion center [36]. It can be seen that in our case the emission peak at 615 nm is stronger than other peaks, indicating that Eu^{3+} ions occupy the asymmetry sites. In addition, the predominant emission peak at 615 nm is favorable to the high purity of red color. As we all known, the properties of materials are strongly dependent on their sizes and morphologies. Under identical measurement conditions, the EuMA with ellipse-like morphology had the highest relative emission intensity, while the samples with plate-like morphology exhibited the lowest intensity. This interesting phenomenon might arise from the difference in the surface defect effects as a consequence of the different sizes of the three samples.

Conclusion

In conclusion, ellipse-like Eu-based metal organic frameworks were successfully synthesized at room temperature without using any template. According to FTIR, XRD and EA analysis, the structure of product is $[Eu(MA)_{1.5}(H_2O)_2]\bullet 5H_2O$. The final morphologies and sizes of the microcrystals can be easily controlled by MA/KOH molar ratio and surfactant. Therefore, 3D ellipse-like, flower-like, plate-like hierarchical architectures were prepared. The investigation of morphology-dependent photoluminescence properties reveals that the ellipse-like samples exhibits the strongest red emission, while the emission intensity of plate-like samples with the smaller size is the lowest, which may be ascribed to the grain size and the amount of defects. This simple morphology-control synthesis strategy could be extended for the preparation of other functional metal–organic framework microstructures, and the obtained 3D architectures could be introduced as the building block for novel optoelectronic devices.

Acknowledgement

The authors gratefully acknowledge the financial support for this work from the National Science Foundation of China (NSFC, No. 51551202), the Scientific Research Fund of Sichuan Provincial Education Department of Sichuan Province (18ZA0408), and the Applied Basic Research Fund of Science & Technology Department of Sichuan Province (No. 2015JY0274).

References

1. Lin YW, Jian BR, Huang SC, Huang CH, Hsu KF (2010) "Synthesis and Characterization of Three Ytterbium Coordination Polymers Featuring Various Cationic Species and a Luminescence Study of a Terbium Analogue With Open Channels".Inorganic Chemistry 49: 2316-2324.
2. Carné-Sánchez A, Imaz I, Stylianou KC, Maspoch D (2014) "Metal-Organic Frameworks: From Molecules/Metal Ions to Crystals to Superstructures".Chemistry - A European Journal 20: 5192-5201.
3. Qin SJ, Hao JN, Xu XY, Lian X, Yan B (2017) "Highly sensing probe for biological metabolite of benzene series pollutants based on recyclable Eu^{3+} functionalized metal-organic frameworks hybrids".Sensors and Actuators B: Chemical 253: 852-859.
4. Lu HY, Tsai MH (2015) "The High-Temperature Synthesis of the Nanoscaled White-Light Phosphors Applied in the White-Light LEDs".Advances in Materials Science and Engineering 2015: 1-6.
5. Kreno LE, Leong K, Farha OK, Allendorf M, Van Duyne RP, et al. (2011) "Metal–Organic Framework Materials as Chemical Sensors".Chemical Reviews 112: 1105-1125.
6. Zhou JM, Shi W, Li HM, Li H,Cheng P (2014) "Experimental Studies and Mechanism Analysis of High-Sensitivity Luminescent Sensing of Pollutional Small Molecules and Ions in Ln_4O_4 Cluster Based Microporous Metal–Organic Frameworks". The Journal of Physical Chemistry C 118: 416-426.
7. Weng H, Yan B (2017) "A sliver ion fabricated lanthanide complex as a luminescent sensor for aspartic acid". Sensors and Actuators B: Chemical 253: 1006-1011.
8. Einkauf JD, Clark JM, Paulive A, Tanner GP, de Lill DT (2017) "A General Model of Sensitized Luminescence in Lanthanide-Based Coordination Polymers and Metal–Organic Framework Materials".Inorganic Chemistry 56: 5544-5552.
9. Yang ZR, Wang MM, Wang XS, Yin XB (2017) "Boric-Acid-Functional Lanthanide Metal–Organic Frameworks for Selective Ratiometric Fluorescence Detection of Fluoride Ions". Analytical Chemistry 89: 1930-1936.
10. Hao J, Liu F, Liu N, Zeng M, Song Y, et al. (2017) "Ratiometric fluorescent detection of Cu^{2+} with carbon dots chelated Eu-based metal-organic frameworks".Sensors and Actuators B: Chemical 245:641-647.
11. Jin SS, Han X, Yang J, Zhang HM, Liu XL, et al. (2017) "Luminescent coordination polymers based on a new resorcin

[4] arene-functionalized tetracarboxylate: Highly selective luminescent detection of metal cations, anions and small organic molecules".Journal of Luminescence 188: 346-355.
12. XingGe, Zhang Y, Cao X (2017) "Bifunctional 3D porous Cu(I) metal-organic framework with gas sorption and luminescent properties".Journal of Molecular Structure 1146: 793-796.
13. XuXY, Yan B (2016) "Fabrication and application of a ratiometric and colorimetric fluorescent probe for Hg^{2+} based on dual-emissive metal–organic framework hybrids with carbon dots and Eu^{3+}".J Mater Chem C4: 1543-1549.
14. Chen H, Liu PX, Zhuo SP, Meng X, Zhou ZY, et al. (2016) "A [Cu 4 I] cluster based metal-organic framework to detect F− ions".Inorganic Chemistry Communications 63: 69-73.
15. Qiu SC, Li Q, Chen K, Zhang YQ, Zhu QJ, et al. (2016) "Absorption properties of an inverted cucurbit[7]uril-based porous coordination polymer induced by [ZnCl4]2− anions". Inorganic Chemistry Communications72: 50-53.
16. XueSF, Lu LF, Wang QX, Zhang S, Zhang M, et al. (2016) "An integrated logic system for time-resolved fluorescent "turn-on" detection of cysteine and histidine base on terbium (III) coordination polymer–copper (II) ensemble".Talanta158: 208-213.
17. Lin XM, Niu JL, Wen PX, Pang Y, Hu L, et al. (2016) "A Polyhedral Metal–Organic Framework Based on Supramolecular Building Blocks: Catalysis and Luminescent Sensing of Solvent Molecules".Crystal Growth & Design 16: 4705-4710.
18. Ma R, Chen Z, Wang S, Yao Q, Li Y, et al. (2017) "Solvent-induced assembly of two helical Eu(III) metal-organic frameworks and fluorescence sensing activities towards nitrobenzene and Cu^{2+} ions".Journal of Solid State Chemistry 252: 142-151.
19. Ma B, Xu J, Qi H, Sun J, Chai J, et al. (2018) "Two 3D metal−organic frameworks as multi-functional materials to detect Fe^{3+} ions and nitroaromatic explosives and to encapsulate Ln^{3+} ions for white-light emission".Journal of Solid State Chemistry 258: 42-48.
20. Xu J, Su D, Bao W, Zhao Y, Xie X, et al. (2016) "Rose flower-like $NiCo_2O_4$ with hierarchically porous structures for highly reversible lithium storage".Journal of Alloys and Compounds 684: 691-698.
21. Chandra D, Dutta A, Bhaumik A (2009) "A New Organic-Inorganic Hybrid Supermicroporous Material Having Luminescence and Ion-Exchange Property".European Journal of Inorganic Chemistry2009: 4062-4068.
22. Lian X, Miao T, Xu X, Zhang C, Yan B (2017) "Eu^{3+} functionalized Sc-MOFs: Turn-on fluorescent switch for ppb-level biomarker of plastic pollutant polystyrene in serum and urine and on-site detection by smartphone".Biosensors and Bioelectronics 97: 299-304.
23. Schaeffer N, Feng X, Grimes S, Cheeseman C (2017) "Recovery of an yttrium europium oxide phosphor from waste fluorescent tubes using a Brønsted acidic ionic liquid, 1-methylimidazolium hydrogen sulfate".Journal of Chemical Technology & Biotechnology 92: 2731-2738.
24. Rosu C, Russo PS, Daly WH, Cueto R, Pople JA, et al. (2015) "Sugar-Based Polyamides: Self-Organization in Strong Polar Organic Solvents".Biomacromolecules 16: 3062-3072.
25. Wang W, Wan W, Stachiw A, Li ADQ (2005) "Foldamers with Hybrid Biological and Synthetic Sequences as Selective DNA Fluorescent Probes".Biochemistry 44: 10751-10756.
26. Ferrari E,Saladini M (2004) "Iron(III) complexing ability of carbohydrate derivatives".Journal of Inorganic Biochemistry 98: 1002-1008.
27. Lakatos A, Bertani R, Kiss T, Venzo A, Casarin M, et al. (2004) "AlIII Ion Complexes of Saccharic Acid and Mucic Acid: A Solution and Solid-State Study".Chemistry - A European Journal 10: 1281-1290.
28. Saladini M, Ferrari E, Menabue L (2002) "Co-ordination of transition metal ions by galactaric acid: a potentiometric and spectroscopic study".Inorganic Biochemistry 92: 121-127.
29. Abrahams BF, Moylan M, Orchard SD, Robson R (2003) "AlIII Ion Complexes of Saccharic Acid and Mucic Acid: A Solution and Solid-State Study".AngewandteChemie 115: 1892-1895.
30. Tian W, Liao aH, WuaJG, Yang GD (1996) "Study on the coordination of the hydroxyl group: crystal structure and FT-IR spectra of potassium hydrogen galactarate ".Polyhedron.16: 2055-2058.
31. Tian W, Yang LM, Xu YZ, Weng SF, Wu JG (2000) "Sugar interaction with metal ions. FT-IR study on the structure of crystalline galactaric acid and its K^+, NH^{4+}, Ca^{2+}, Ba^{2+}, and La^{3+} compl exes ".Carbohydrate Research 324: 45-52.
32. Wong KL, Law GL, Yang YY, Wong WT (2006) "A Highly Porous Luminescent Terbium–Organic Framework for Reversible Anion Sensing".Advanced Materials 18: 1051-1054.
33. Tian Y, Chen B, Tian B, Yu N, Sun J, et al. (2013) "Hydrothermal synthesis and tunable luminescence of persimmon-like sodium lanthanum tungstate:Tb^{3+}, Eu^{3+} hierarchical microarchitectures". Journal of Colloid and Interface Science 393: 44-52.
34. Kumar Y, Pal M, Herrera M, Mathew X (2016) "Effect of Eu ion incorporation on the emission behavior of Y_2O_3 nanophosphors: A detailed study of structural and optical properties".Optical Materials 60: 159-168.
35. García CR, Oliva J, Romero MT, Ochoa-Valiente R, Garcia Trujillo LA (2015) "Effect of Eu^{3+} Concentration on the Luminescent Properties of $SrTiO_3$ Phosphors Prepared by Pressure-Assisted Combustion Synthesis".Advances in Materials Science and Engineering 2015: 1-5.
36. Gu Q, Chu N, Pan G, Sun G, Ma S, et al. (2014) "Intercalation of Diverse Organic Guests into Layered Europium Hydroxides - Structural Tuning and Photoluminescence Behavior".European Journal of Inorganic Chemistry 2014: 559-566.